Ab Initio Calculations of Structural Evolution and Conductance of Benzene-1,4-dithiol on Gold Leads

Renato Borges Pontes,[†] Alexandre Reily Rocha,[‡] Stefano Sanvito,[§] Adalberto Fazzio,[†] and Antônio José Roque da Silva*[,†,⊥]

[†]Instituto de Física, Universidade de São Paulo, CP 66318, 05315-970, São Paulo, SP, Brazil, [‡]Centro de Ciências Naturais e Humanas, Universidade Federal do ABC, Santo André, SP, Brazil, [§]School of Physics and CRANN, Trinity College, Dublin 2, Ireland, and [⊥]Laboratório Nacional de Luz Síncrotron, CP 6192, 13083-970, Campinas, SP, Brazil

ABSTRACT By performing *ab initio* density functional theory (DFT) calculations and electronic transport simulations based on the DFT nonequilibrium Green's functions method we investigate how the conformational changes of a benzene-1,4-dithiol molecule bonded to gold affect the molecular transport as the electrodes are separated from each other. In particular we consider the full evolution of the stretching process until the junction breaking point and compare results obtained with a standard semilocal exchange and correlation functional to those computed with a self-interaction corrected method. We conclude that the inclusion of self-interaction corrections is fundamental for describing both the molecule conductance and its stability against conformational fluctuations.

KEYWORDS: molecular electronics · density functional theory · transport calculations · self-interaction correction

Molecular electronics,[1,2] where organic molecules provide the active element of an electronic device, is one of the most promising technologies potentially able to meet the requirements of device miniaturization at the end of the Si roadmap. Although in the past few years a continuous effort has been dedicated to making stable and reproducible molecular devices, the lack of control in the fabrication process has limited the progress. Since the pioneering work of Reed *et al.*,[3] who first measured, by mechanically controllable break junctions (MCBJ), the conductance of a single benzene-1,4-dithiol (BDT) molecule attached to a gold surfaces, BDT has been considered the benchmark molecule for both theoretical[4−12] and experimental studies.[13−17] However, even for this simple molecule the disagreement between theory and experiments and even among seemingly similar experiments remains large.[18]

The most recurrent explanation given to account for such discrepancies is the lack of knowledge of the microscopic details of the contact region between the molecule and the electrodes.[9,17] In fact, only rarely one knows how the BDT binds to the electrodes, what is the preferential absorption site, and how is the molecule oriented with respect to the surface. An additional complication arises from the fact that all these features may change with the molecular coverage in self-assembled monolayers. A second possible explanation for the differences between theory and experiments is that the present level of theoretical description, based on local and semilocal density functional theory (DFT) and Landauer quantum transport, may be inadequate. This problem was addressed by Toher *et al.*,[19,20] who showed that theoretical predictions are in much closer agreement with experiments when self-interaction corrected exchange and correlation functionals are employed.

One of the most established techniques to investigate electron transport in molecular devices relies on conducting statistical experiments based on breaking junctions or scanning tunneling microscopy (STM).[13] In these, two electrodes are moved into and out of contact in the presence of the desired molecules. During the approach, molecules can bridge the gap between between the electrodes and form a junction. Such a junction is then modified during the retraction, so that in practice one measures a collection of molecular devices at once, each one corresponding to a different electrodes separation. As such, statistical molecular device experiments provide a much more rich set of data about the conductance of a molecule. In particular the dependence of the electrical characteristic on the electrodes separation can help in understanding the stability of a particular molecular junction. Ideally one wants to reproduce these statistical experiments theoretically, so that

*Address correspondence to pontes@if.usp.br, ajrsilva@if.usp.br.

Received for review July 13, 2010 and accepted December 22, 2010.

Published online January 12, 2011
10.1021/nn101628w

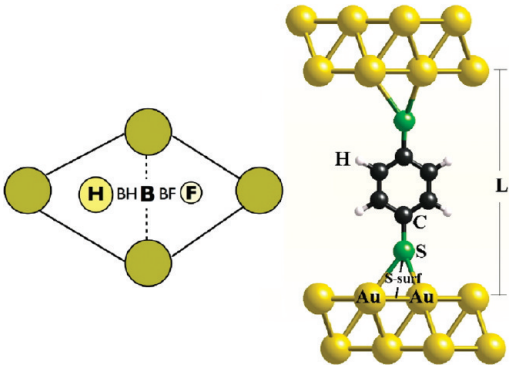

Figure 1. Left panel: Adsorption sites for BDF on an Au(111) surface: H, BH, B, BF and F stand for hcp, bridge−hcp, bridge, bridge−fcc, and fcc sites, respectively. Right panel: Schematic representation of BDT on gold leads. *L* is the lead−lead separation. The distances presented in Table 1 are also shown.

the errors introduced by the theoretical method chosen can be singled out from the uncertainty over the atomic configuration of the device. This is the goal of our work.

We perform a systematic investigation of the evolution of the conductance of a BDT molecule as the separation between the electrodes reaches the junction breaking point. In particular we compare calculations performed with the standard Perdew−Burke−Ernzerhof generalized gradient approximation (PBE-GGA)[21] to the exchange and correlation functional with those obtained by using an approximate self-interaction correction scheme (ASIC)[22,23] to the local density approximation (LDA). The main effect of the ASIC is to partially position the Kohn−Sham highest occupied molecular orbital (HOMO) close to the negative of the molecule true ionization potential. This feature is absent in both the LDA and GGA, where the HOMO is typically too high. Note that for the molecule investigated here GGA and LDA give qualitatively similar results so that we have decided to present results for GGA only.

RESULTS AND DISCUSSION

We start our investigation of the evolution of a Au/BDT/Au junction by looking at two possible conformations. In the first BDT is adsorbed at an fcc site (F) perpendicular to the gold electrodes, and in the second the molecule is adsorbed at a bridge−fcc site (B) almost parallel to the gold surface (see Figure 1). The parallel configuration is energetically more stable for low coverage, although both structures are possible depending on the experimental conditions and the electrodes separation. We perform our calculations by assuming a low-coverage situation, where BDT molecules are far enough not to interact with each other.

The two initial conformations are taken from previous calculations.[4] Then, both the junctions are stretched by pulling the electrodes apart and by relaxing the junction geometry at each step in the pulling.

TABLE 1. Structural Properties and Transmission Coefficient at the Fermi Level, $T(E_F)$, for BDT Perpendicular to the Au Leads[a]

structure	d_{S-surf}	d_{Au-S}	d_{S-C}	L	ΔE	$T(E_F)$	$T^{ASIC}(E_F)$
a	1.61	2.51	1.78	9.78	0.04	0.41	0.07
b	1.78	2.56	1.78	10.18	0.00	0.51	0.05
c	1.96	2.64	1.79	10.58	0.08	0.65	0.06
d	2.16	2.75	1.80	10.98	0.26	0.87	0.07
e	2.35	2.86	1.79	11.38	0.51	1.00	0.14
f	2.57	3.02	1.76	11.78	0.76	0.78	0.28
g	2.79	3.20	1.74	12.18	0.98	0.39	0.12

[a] The distances d_{S-surf}, d_{Au-S}, and d_{S-C} are defined in Figure 1 (right panel). L is the separation between the leads. The values of d and L are given in Å. ΔE is the cell total energy calculated with respect to that of the most stable configuration.

The relaxation is carried out by PBE-GGA conjugate gradient, and the relaxed atomic configurations are then used for both the GGA and ASIC transport calculations. Note that the ASIC method is only approximately variational[22,23] so that ASIC atomic relaxation at this time is not possible. However, since the ASIC mostly corrects the Kohn−Sham eigenvalues but little the total energy and the electron density, we expect that the GGA geometries may be a good approximation of the ASIC ones. More details about the relaxation are provided in the Computational Methods Section.

Perpendicular BDT Conformation. The geometry in which BDT is oriented perpendicularly to the Au surface is the most studied in literature[3,24] and also the starting point of our analysis. The structural properties of this configuration as a function of the leads separation, L, are summarized in Table 1, where we report the calculated values for the various bond lengths, for the cell total energy, and for the transmission coefficient at the Fermi level, E_F (both calculated with GGA and ASIC). We find that the most energetically stable structure occurs for a lead−lead separation of 10.18 Å. For such a distance the calculated bond length between the S atom and the surface layer (d_{S-surf}) is 1.78 Å, which is in good agreement with previous theoretical calculations.[8,10] Note that the S−Au surface bond length is the most affected by the stretching process, while the S−C bond lengths (d_{S-C}) do not change significantly.

In Figure 2a, b we present the cell total energy and the pulling force (see the Computational Methods Section for a rigorous definition of the pulling force) as a function of the electrodes separation. The reference energy is chosen to be that of the lowest-energy structure (for L = 10.18 Å). The maximum achieved force just before the rupture of the Au−S bond is calculated to be 1.1 nN. For the points indicated as (a−g) over the total energy curve we have also performed electronic transport calculations, and a representative set of GGA transmission coefficients as a function of energy is presented in the lower panels of Figure 2. From the figure one can immediately observe that the GGA transmission at E_F increases steadily from

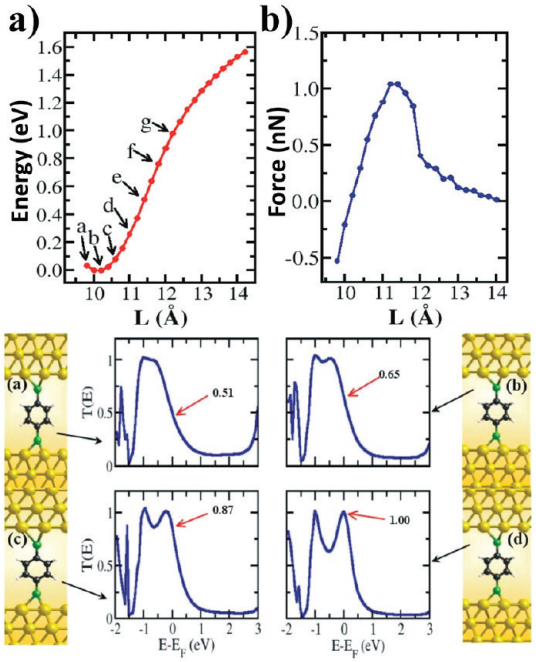

Figure 2. Upper panel: Total energy (a) and the pulling force acting on the system (b) calculated along the various steps of the stretching process. The total energy values are displayed relatively to the lowest-energy structure, shown in Figure 1c. The results are presented as a function of the electrodes separation, *L*. Lower panel: Transmission coefficient as a function of energy and atomic geometries of BDT adsorded at the fcc site for a lead−lead separation, respectivel,y of 10.18, 10.58, 10.98, and 11.38 Å.

0.51 at the equilibrium lead−lead separation to approximately 1.0 at L = 11.38 Å, *i.e.*, for an electrode gap elongation of about 1 Å. Then for separations larger than 11.38 Å, $T(E_F)$ starts decreasing.

The initial increase of $T(E_F)$ with L can be easily understood by looking at the projected density of state (PDOS) of the system, presented in Figure 3. We observe a movement of the S p-derived BDT HOMO toward higher energies as the junction is stretched. This brings the HOMO toward a perfect alignment with the Au Fermi level, meaning that the reduction in electronic coupling between the BDT and the electrodes induced by the elongation of the Au−S bond is completely compensated by a realignment of the molecular levels. Such a mechanism has been already proposed for the same molecule in the literature.[8,20] Finally for L larger than 11.38 Å, the stretching of the S−Au bond is no longer compensated by a realignment of the molecular levels with the Fermi energy, and thus the conductance decreases.

When SIC are taken into account the picture described above changes considerably. The upper panel of Figure 4 compares the zero-bias transmission coefficient, $T(E_F)$, for both GGA and ASIC, while the lower panel of the same figure presents the ASIC calculated $T(E)$ for two different lead−lead separation. The most important and remarkable feature (see also Table 1) is the systematic reduction of the ASIC transmission at

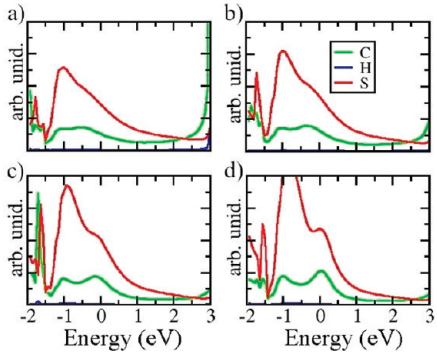

Figure 3. PDOS for Au/BDT/Au calculated for different electrodes separation: (a) 10.18, (b) 10.58, (c) 10.98, and (d) 11.38 Å (see Figure 2).

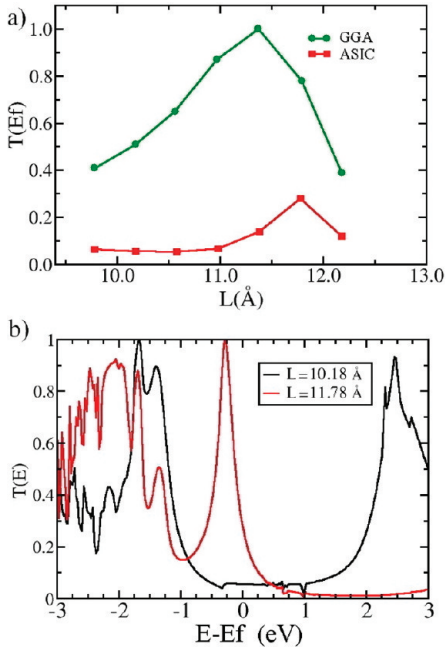

Figure 4. (a) ASIC and GGA calculated transmission coefficients for BDT in the perpendicular configuration as a function of the electrodes separation. (b) ASIC transmission coefficients for different stretching distances.

the Fermi level with respect to the GGA one. This persists for all the lead−lead separations investigated. In particular we find a zero-bias conductance for the most stable configuration of 0.05 G_0 ($G_0 = 2e^2/h$ is the quantum conductance, e the electron charge, and h the Planck constant), which is of the same order of magnitude as that measured by Xiao *et al.*[13] and is in good agreement with previously published results.[20]

A second important feature of the ASIC results is that the transmission is much less sensitive to variations in the bond length than its GGA counterpart. In fact the ASIC transmission as a function of L is almost constant up to L = 11 Å. This feature is a clear indication that self-interaction corrections are not only important in order to obtain the correct value for the conductance but also for describing the stability of the conductance curve during the stretching process, a stability which is

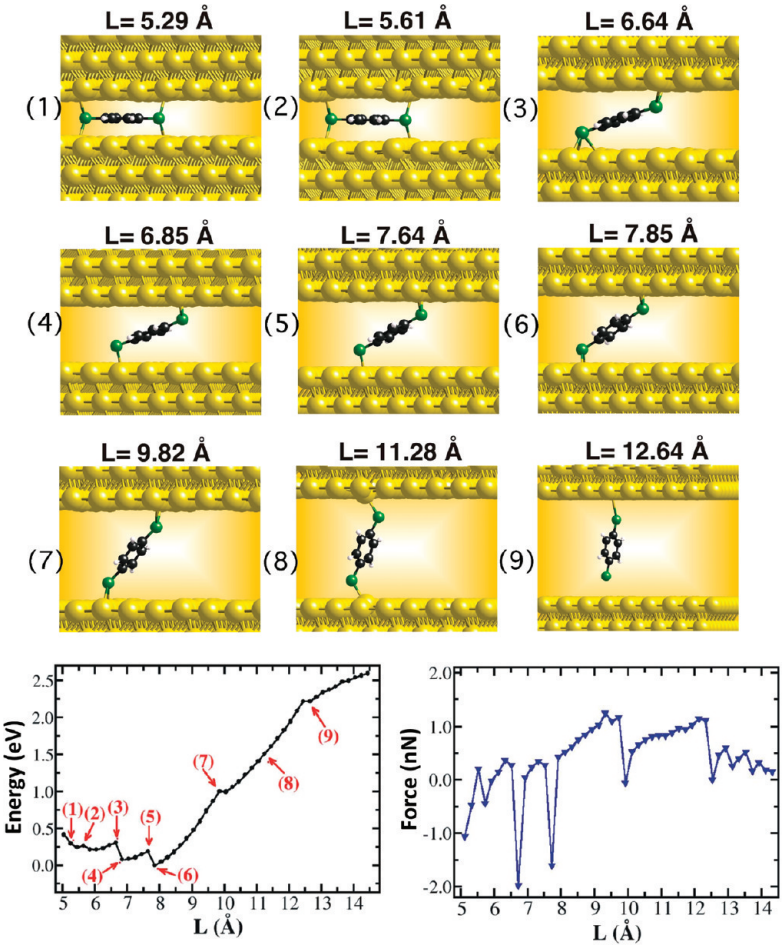

Figure 5. Upper panel: Graphics of the different stages of the evolution of BDT on gold during a MCBJ experiment. The initial configuration is that of a flat BDT molecule on the surface. *L* is the leads separation at each stage. Lower panel: Total energy and pulling force as a function of the leads separation. The total energy values are displayed relative to the lowest-energy structure (structure 6).

observed in experiments.[13] Finally as the lead−lead separation approaches the rupture point, $T(E_F)$ starts increasing also when calculated with ASIC.

The effects of the SIC on the transport can be appreciated by comparing $T(E)$ for L = 10.18 Å, calculated with GGA (see Figure 2) and ASIC (see Figure 4). The main difference between the two calculations is the position of the S-derived HOMO with respect to the electrode Fermi level. In the case of GGA this is approximately 0.5 eV below E_F, but since there is strong electronic coupling between the BDT and the electrodes, its contribution to the transmission at the Fermi level is significant. The ASIC pushes such a peak downward in energy and away from the Fermi level by about 1 eV. The transport is now tunneling-like since the electrode Fermi level is placed within the highest occupied and lowest unoccupied molecular orbitals (HOMO−LUMO) gap of the molecule.

Such a behavior of the ASIC functional is rooted in its much better description of the BDT ionization potential in terms of Kohn−Sham eigenvalue. In fact the ASIC calculated HOMO for the BDT molecule in the gas phase is around −8.5 eV, in good agreement with the experimentally available values for the ionization potential.[20] In contrast the GGA HOMO is only about −5 eV, *i.e.*, it is about 3 eV too shallow. This means that the GGA HOMO will be much closer to the Au Fermi level (also around −5 eV) than the ASIC one. In summary the effects of the SIC is that of changing the transport through the BDT from resonant at the HOMO level (this is the case for GGA) to tunneling-like.

Flat BDT Conformation. A more realistic description of a STM/MCBJ experiment is obtained by performing a full stretching simulation, where one of the two electrodes first approaches a molecule on a surface, then makes contact and finally pulls away. This is what we calculate next by starting from the energetically most stable structure previously calculated for a single molecule on a single Au(111) surface,[4] in which BDT orients almost parallel to the surface.

The evolution of the Au/BDT/Au structure in the junction breaking process as a function of lead−lead distance can be monitored in Figure 5, where we present nine representative geometries calculated respectively

for nine different electrodes separations. For small L (Figure 5, panels 1 and 2) the BDT interacts strongly with both the gold surfaces, and an almost parallel conformation remains stable until L reaches 5.61 Å (first elastic stage). Already at the next separation considered (5.82 Å) the situation changes, and the molecule begins to tilt away from the Au(111) plane (second elastic stage). As the lead−lead distance is increased between 6.85 and 7.64 Å (Figure 5, panels 4 and 5), the molecule tilts more and drifts along the Au surface until forming a single atom bond with Au (third elastic stage). At the lowest-energy configuration (Figure 5, panel 6) BDT is finally adsorbed at a bridge−fcc site, it presents a tilting angle of approximately 57.8°, and the Au−S distance is 2.6 Å. With further stretching (fourth elastic stage in Figure 5, panel 6) the tilting angle changes roughly by about 10°, and the molecule moves to an upright geometry. Finally in the last elastic stage (Figure 5, panels 7 and 8) the molecule tilts even further and now attaches to only one atom at each surface. At this point the bridge configuration is broken. During this final stage, upon increasing the leads distance the Au atom connecting to the BDT is displaced outside the Au(111) plane in an attempt to maximize its interaction with both the Au surface and the BDT, until the Au−S bond eventually snaps for L = 12.64 Å (Figure 5, panel 9). Note that during this evolution the BDT intramolecular bonds do not change significantly.

In Figure 5 we also present the total energy and the pulling force as a function of the electrodes' separation. The dynamical evolution of the forces with L shows a behavior more complex than that of the perpendicular conformation. This is due to reconstructions and bond breaking which are not present for the previous structure. In particular the pulling force as a function of L is characterized by elastics stages (where the force increases) followed by stress release. The existence of negative forces means that the system is under compressive strain. We calculate a value for the applied force just before the breaking point of 1.1 nN corresponding to a maximum Au−S distance of about 2.86 Å. Such a force is marginally smaller than that measured with an atomic force microscope for polysaccharide molecules[25] (∼1.4 ± 0.3 nN). Given the complexity of these experiments, we believe that the agreement is rather satisfactory and within experimental error.

Additionally, as discussed by Kruger *et al.*,[26,27] the difference could be associated to the fact that experimentally[25] the rupture might occur between a different bond than Au−S (for instance between two Au atoms). Our calculations show that such a situation will not happen when starting from two perfectly flat surfaces but might arise if the molecule binds to an under-coordinated Au atom, which could change the Au−S rupture force due to the modification of the local conformation. Another point, there is no certainty that different molecules (polysaccharide in experiments and BDT in theory) will break the Au−S bond at an identical pulling force, since the geometry before the rupture point may be different. Finally, some of the disagreement may arise from the calculations themselves, which depend on the choice of exchange and correlation potential, initial geometry, *etc.*[28]

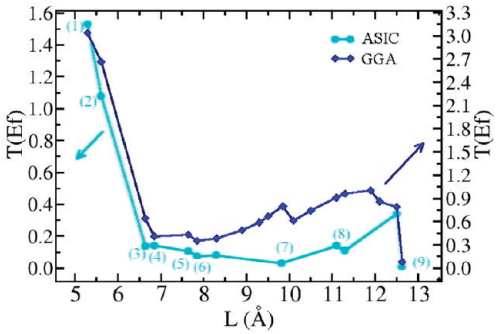

Figure 6. GGA and ASIC transmission coefficient at the Fermi level calculated for BDT in the flat initial configuration as a function of the lead−lead separation.

The variation of the conductance as a function of the lead−lead separation is presented next in Figure 6 for both the GGA and the ASIC. Let us start by commenting on the GGA results. We note that for small separations $T(E_F)$ is quite large (3.04 and 2.66, respectively, for L = 5.29 and 5.61 Å). This is because in the parallel conformation all of the p_z orbitals (associated to either S or C) interact strongly with the electrodes and produce high transmission. As the molecule reaches a more upright position, $T(E_F)$ becomes similar to that of the perpendicular configuration, *i.e.*, the transmission is resonant through the BDT HOMO. The actual position and broadening of the HOMO peak are determined by the details of the bonding geometry, and $T(E_F)$ varies between 0.41 for L = 6.64 Å to approximately 1.0 just before the junction breaking.

This scenario is qualitatively maintained in the ASIC calculations, with a rather large $T(E_F)$ for small separations (1.6 and 0.99, respectively, for L = 5.29 and 5.61 Å), a drastic reduction at the onset of the upright configuration followed by a smooth increase just before the rupture. Hence the main difference between GGA and ASIC is simply in the magnitude of the transmission, which is about a factor of five smaller for ASIC than for GGA. Again the reason for this difference originates from the ASIC shift of the HOMO away from the electrode Fermi level, so that the ASIC transport is mainly *via* tunneling through the BDT HOMO−LUMO gap. Notably the increase in conductance just before the rupture point, also present in ASIC, has precisely the same origin to that discussed for the perpendicular case, *i.e.*, it is due to a realignment of the HOMO level, which is not compensated by a reduction in the level broadening.

Finally in Figure 7 we summarize our results by plotting together the GGA pulling forces and the ASIC transmission at the Fermi level as a function of the lead−lead separation. We note, in agreement with

experimental measurements, that the conductance remains rather stable for a rather large range of electrode separation, despite the fact that the force goes through a number of sharp changes.

Double BDT Junction. Another possible scenario that might arise in MCBJ experiments is the one where two BDT molecules are sandwiched between the electrodes, *i.e.*, where both the Au surfaces are decorated with flat BDTs. This geometry was suggested a long time ago[29] in order to explain the low value of conductance measured by Reed *et al.*[3] Also for this case we have followed the evolution of the junction as the electrodes are pulled apart by starting from the most energetically stable geometry, which is rather similar to that of a single BDT simply adsorbed on the Au surface.[4]

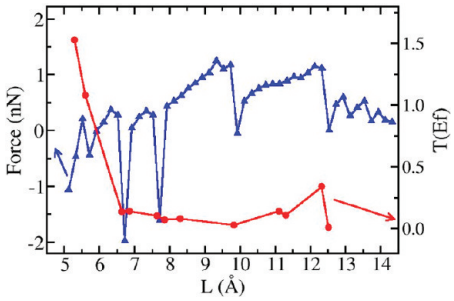

Figure 7. GGA pulling force and ASIC transmission coefficient at the Fermi level calculated for the BDT in the flat initial configuration as a function of the lead−lead separation.

Four representative geometries along the pulling curve together with the cell total energy and the pulling force as a function of L are presented in Figure 8. We find that the rupture force is only 0.05 nN, *i.e.*, it is considerably smaller than the one measured for the Au−S bond.[25] This corresponds to the breaking of the van der Waals interaction between the two benzene rings of the two BDT molecules. Note that the systematic lack of a precise description of van der Waals interaction in GGA in this case may produce a rather large error in the calculated pulling force, which nevertheless is expected to be small. This suggests that the two-molecule geometry is unlikely to appear in MCBJ experiments. Such a consideration is supported by the conductance calculations. We find that the zero-bias conductance for the most stable configuration is 0.04 G_0 when calculated with GGA and 0.002 G_0 for ASIC (see Figure 11b). Interestingly the GGA conductance is still larger than that measured by Xiao *et al.* (0.011 G_0) in well-controlled statistical experiments,[13] but both the GGA and ASIC conductances are at least one order of magnitude larger than that measured first by Reed *et al.*[3] This seems to suggest that the two-molecule configuration may not play a particular role in MCBJ

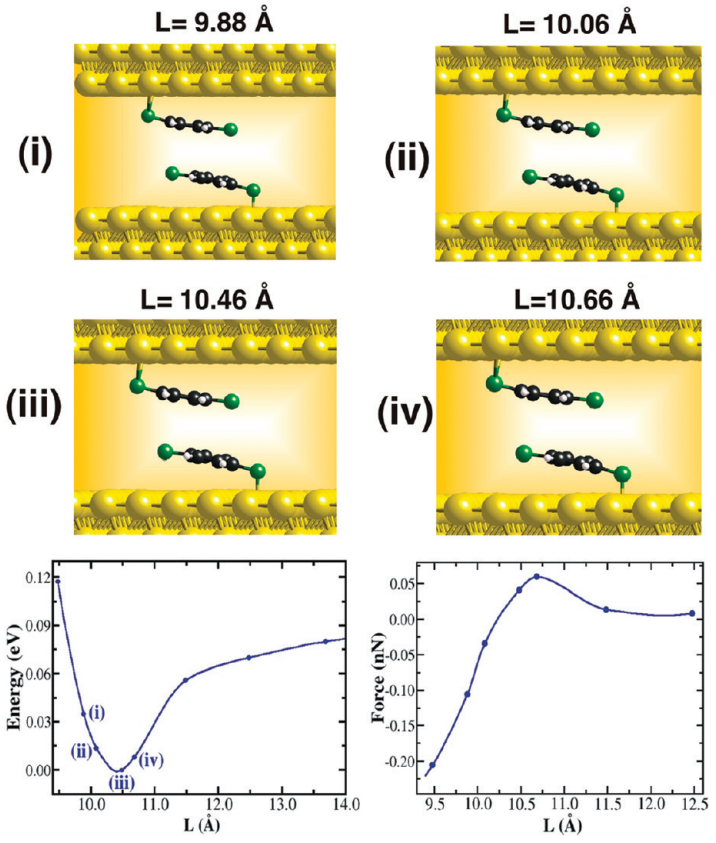

Figure 8. Structural properties of the two BDT junction. In the upper panels, four representative geometries corresponding to four different electrodes' separations, L. These structures are then used for the transport calculations. In the lower panels, the respective cell total energy and the pulling force as a function of L. The reference total energy is chosen to be that of the lowest-energy configuration.

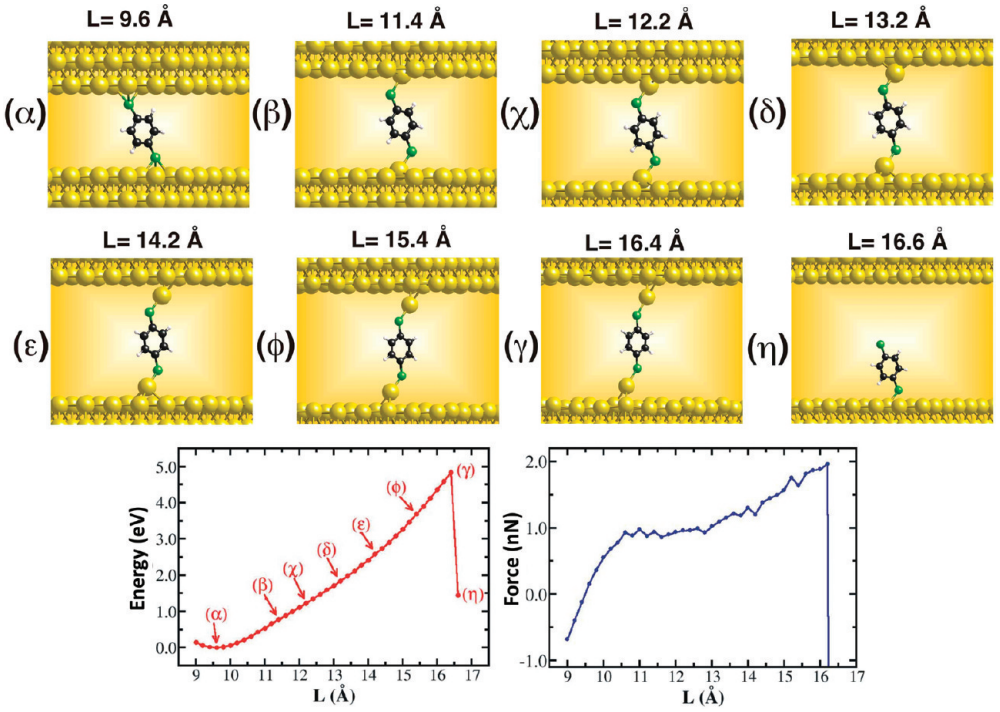

Figure 9. Geometries obtained for a BDT molecule attached to Au electrodes at an initial tilting angle during the pulling process. In the lower panels, the cell total energy and the pulling force as a function of the leads separation, *L*. The reference total energy is that of the equilibrium conformation.

experiments, *i.e.*, it is not a statistically relevant configuration.

Tilted BDT Configuration. The final configuration investigated is a variation of the perpendicular one, which was addressed first. In this case, however, the molecule makes an initial bond to Au at an angle with respect to the (111) surface. One then expects that further stress may be released by first rotating the molecule toward the vertical direction. The simulated stretching is presented in Figure 9. The most interesting feature is that the tilting angle is maintained during the pulling of the electrodes (although it gets reduced as *L* increases), and additional elongation is possible by pulling a Au atom significantly outside the surface. As such, the rupture distance is calculated to be 16.6 Å, *i.e.*, it is significantly larger than 12.6 Å calculated for a stretching process initiated from the bridge−fcc conformation.

The cell total energy and the pulling force calculated as a function of the electrodes' separation (see Figure 9) reveal an elastic behavior followed by a sudden rupture but no indication of stress release. Interestingly the calculated rupture force is 2.0 nN, *i.e.*, it is considerably larger than the rupture forces obtained for all the other configurations. We attribute such an enhanced rupture force to the fact that the last bond broken is between S and a single Au atom.

In Figure 10 the energetics for all the geometries studied are compared. We find that for small leads separation BDT prefers the bridge−fcc conformation, which becomes less energetically stable for $L > 9.82$ Å,

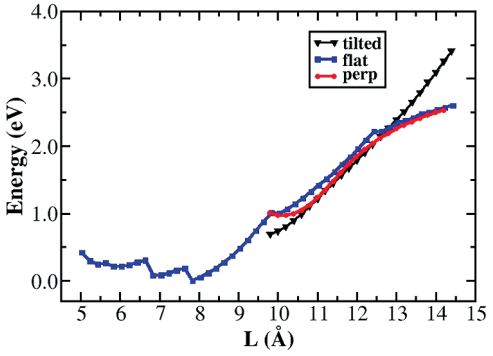

Figure 10. Variation of the total energy as a function of the leads separation for all the single BDT structures investigated: perpendicular, flat, and tilted. The reference energy is the lowest-total energy for the BDT flat configuration.

where the tilted geometry presents a lower energy. We note however that the energy difference among these conformations is small, which explains why it is so difficult to experimentally determine unequivocally the molecular geometry of the junction.

Finally in Figure 11 we summarize all the zero-bias $T(E_F)$ calculated for the various configurations as a function of *L*. In particular we present results for GGA and ASIC (Figure 11, upper and lower panels, respectively). Overall we find two main features brought by the ASIC. First the ASIC conductance is systematically lower than that of the GGA, essentially for all the geometries and electrodes' separations investigated. Second the ASIC calculated values seem to be much less sensitive to the details of the bonding geometry between BDT and Au (except for the situation where

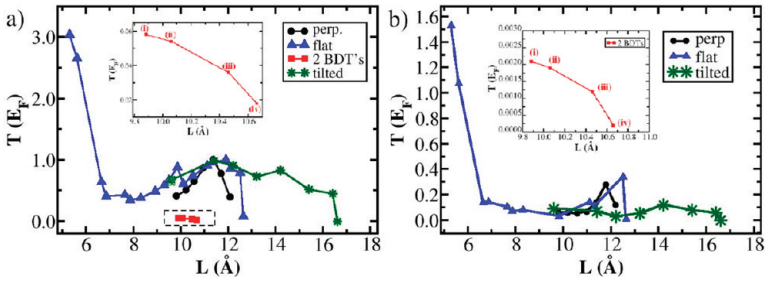

Figure 11. Transmission coefficients calculated at the Fermi level as a function of the electrodes' separation for all the geometries investigated: (a) GGA results, and (b) ASIC. The insets displays $T(E_F)$ for two-molecule conformation.

BDT is flat on the surface). Both these results originate from the fact that the ASIC transmission is not resonant through the HOMO, but it is simply tunneling-like, being the electrodes Fermi level sitting approximately in the middle of the HOMO−LUMO gap. These features are in much better agreement with the statistical experiments of Xiao *et al.*[13] and remark the importance of correcting local and semilocal exchange and correlation functionals in order to make transport calculations reliable.

CONCLUSIONS

In conclusion, we have used state-of-the-art *ab initio* density functional theory calculations to systematically investigate the stretching process of a MCBJ incorporating a BDT molecule. In particular, we have reviewed a number of different cases corresponding to different initial configurations of the junction. The total energy and the pulling forces are computed at the GGA level, and then zero-bias transport simulations are performed with both GGA and ASIC. In general we find that a flat geometry, where the BDT is parallel to the Au surface, is the most energetically stable for small electrodes' separations. However the electrodes' pulling process results in BDT contacting the two surfaces with one thiol group attached at each side, *i.e.*, in a configuration that bridges the gap between the two electrodes. The details of these intermediate configurations depends on the initial geometry at the start of the pulling process.

The GGA conductance appears rather sensitive to the different geometries and in general is substantially larger than that measured in statistical experiments. This is because the transport is resonant at the HOMO, whose actual energy position is sensitive to the precise bonding geometry. Such a sensitivity is partially eliminated by the ASIC, since the HOMO is systematically pushed to lower energies. The action of the ASIC on the molecule in the gas phase is that of restoring Koopmans' theorem for the molecular HOMO. For this reason we believe that our ASIC results are more appropriate to describe the real level alignment of the junction and therefore the transport. This indeed seems to be the case, and the average ASIC calculated conductance is only a factor five larger than the accepted experimental value. Furthermore and probably most importantly, the ASIC conductance is much more robust than the GGA one to conformational changes of the junction, *i.e.*, it is more stable with respect to the multiple configurations which are inevitably explored in a statistical experiment.

Finally we wish to remark that some disagreements between theory and experiments persist, namely the fact that even the ASIC conductance is still larger than the experimental one (note that the value of 0.011 G_0 reported by Xiao *et al.*[13] represents one of the largest measured conductances for this molecule). We believe that there might be three reasons for such a disagreement. First it is still possible that the most probable geometries in actual experiments are not among those investigated here. For instance adsorption of BDT at alternative bonding sites can change the conductance. In particular this can be reduced if the bonding occurs asymmetrically at the two electrodes.[19] A second possible reason is that the conductance can be further reduced by the effect of hydration of the molecule,[30] *i.e.*, by the fact that, at variance with what calculated here, the actual experiments are carried out in solution. Finally, a further source of disagreement may arise from the fact that the GGA calculated configurations may be not accurate enough. Improvements on this front requires a fully variational form of the ASIC scheme, which is currently under development.

COMPUTATIONAL METHODS

Our results for the structural evolution of the BDT on gold electrodes are based on first principles total energy DFT calculations.[31,32] We have used the PBE-GGA functional[21] and norm-conserving pseudopotentials,[33] as implemented in the SIESTA code.[34,35] Numerical orbitals were used as basis sets,[36] and we have employed a split-valence double-ζ basis with polarization function (DZP) for the Au layers where the BDT is attached plus the BDT atoms, and for the remaining Au atoms we used a DZ basis set. The confining energy shift was 0.03 eV,

and a cutoff of 250 Ry for the grid integration was used. For the surface Brillouin zone (BZ) sampling we have used a (4,4) Monkhorst−Pack set.[37] We have used periodic boundary conditions and a supercell approximation. To obtain the geometries, the supercell was such that the molecule would be connected to the two sides of the Au slab. The Au slab was modeled by a (3 × 3) surface unit cell and five layers of gold (36 Au atoms). In all calculations the positions of the BDT and Au atoms on first the two layers at either side were allowed to relax until the forces were smaller than 0.03 eV/Å. All other atoms were held fixed at their bulk positions. The separation between the electrodes was increased in steps of 0.2 Å, and for each new supercell length, the system was fully relaxed as described above. This procedure was followed until we identified the rupture of the Au−S bond. The force was calculated as $F_z = (\partial E_{tot}/\partial \Delta L)$, where E_{tot} is the total energy of the system at each stretching and ΔL stands for the elongation of the system.

For the transport calculations we have used the TRANSAMPA[38] and SMEAGOL codes[39] which employ the nonequilibrium Green's function scheme combined with density functional theory (NEGF-DFT).[40−42] In particular, a development version of the SMEAGOL code was used for the calculations including self-interaction corrections, since as discussed previously,[19,20] SIC is found to dramatically correct over local functionals the transport properties of a molecular device. The SIC scheme used is that originally proposed by Filippetti and Spaldin[22] and subsequently implemented in a local basis environment by Pemmaraju *et al.*[23] (This implementation is known as ASIC).

In brief, the ASIC method is a simplified version of the standard Perdew−Zunger SIC construction,[43] where one assumes that the orbitals which minimize the self-interaction energy are simple atomic orbitals. As such, no unitary transformation of the occupied manifold is required to find the SIC energy minimum, and a standard Kohn−Sham procedure can be designed. The resulting ASIC potential is orbital independent and essentially consists of an atomic orbital projector multiplied by the SI energy associated to that given atomic orbital. The net action of such a corrective potential is that of reducing the energy of the Kohn−Sham eigenvalues of the occupied states, while leaving that of the unoccupied ones unchanged. Thus the ASIC method is similar to LDA + *U*, with the two substantial differences that empty states are not corrected and that the Coulomb repulsion *U* is calculated self-consistently.

In all the transport calculations the device region includes the BDT plus five (3 × 3) Au layers on each side. Periodic boundary conditions are employed parallel to the surface, and the Γ-point only is used when sampling the BZ. The calculations are performed with a DZP basis set for the molecule and a DZ basis set for the Au atoms. Here we report data for the conductances only, *i.e.*, we limit our analysis to the linear response only.

Acknowledgment. The authors R.B.P., A.R.R., A.F., and A.J.R. thank the Brazilian agencies FAPESP, CAPES, and CNPq for financial support and CENAPAD-SP for computational time. S.S. thanks the Science Foundation of Ireland (grant 07/IN.1/I945) and CRANN for financial support.

NOTE ADDED AFTER ASAP PUBLICATION

Due to a production error, Figure 10 was published with the wrong artwork. The corrected version was published on January 21, 2011.

REFERENCES AND NOTES

1. Aviram, A.; Ratner, M. A. Molecular Rectifiers. *Chem. Phys. Lett.* **1974,** *29*, 277.
2. Reed, M. A.; Lee, T. *Molecular Nanoelectronics*; American Scientific Publishers: Valencia, CA, 2003.
3. Reed, M. A.; Zhou, C.; Muller, C. J.; Burgin, T. P.; Tour, J. M. Conductance of a Molecular Junction. *Science* **1997,** *278*, 252–254.
4. Pontes, R. B.; Novaes, F. D.; Fazzio, A.; da Silva, A. J. R. Adsorption of Benzene-1,4-dithiol on the Au(111) Surface and Its Possible Role in Molecular Conductance. *J. Am. Chem. Soc.* **2006,** *128*, 8996–8997.
5. Di Ventra, M.; Pantelides, S. T.; Lang, N. D. First-Principles Calculation of Transport Properties of a Molecular Device. *Phys. Rev. Lett.* **2000,** *84*, 979–982.
6. Yaliraki, S. N.; Kemp, M.; Ratner, M. A. Conductance of Molecular Wires: Influence of Molecule-Electrode Binding. *J. Am. Chem. Soc.* **1999,** *121*, 3428–3434.
7. Yaliraki, S. N.; Roitberg, A. E.; Gonzalez, C.; Mujica, V.; Ratner, M. A. The Injecting Energy at Molecule/Metal interfaces: Implications for Conductance of Molecular Junctions from an Ab Initio Molecular Description. *J. Chem. Phys.* **1999,** *111*, 6997–7002.
8. Xue, Y.; Ratner, M. A. Microscopic Study of Electrical Transport through Individual Molecules with Metallic Contacts. II. Effect of the Interface Structure. *Phys. Rev. B: Condens. Matter Mater. Phys.* **2003,** *68*, 115406.
9. Basch, H.; Cohen, R.; Ratner, M. A. Interface Geometry and Molecular Junction Conductance: Geometric Fluctuation and Stochastic Switching. *Nano Lett.* **2005,** *5*, 1668–1675.
10. Stokbro, K.; Taylor, J.; Brandbyge, M.; Mozos, J. -L.; Ordejon, P. Theoretical Study of the Nonlinear Conductance of Di-Thiol Benzene Coupled to Au(111) Surfaces *via* Thiol and Thiolate Bonds. *Comput. Matter. Sci.* **2003,** *27*, 151–160.
11. Geng, W. T.; Nara, J.; Ohno, T. Impacts of Metal Electrode and Molecule Orientation on the Conductance of a Single Molecule. *Appl. Phys. Lett.* **2004,** *85*, 5992–5994.
12. Emberly, E. G.; Kirczenow, G. Models of Electron Transport through Organic Molecular Monolayers Self-Assembled on Nanoscale Metallic Contacts. *Phys. Rev. B: Condens. Matter Mater. Phys.* **2001,** *64*, 235412.
13. Xiao, X. Y.; Xu, B. Q.; Tao, N. J. Measurement of Single Molecule Conductance: Benzenedithiol and Benzenedimethanethiol. *Nano Lett.* **2004,** *4*, 267–271.
14. Dorogi, M.; Gomez, J.; Osifchin, R.; Andres, R. P.; Reifengerger, R. Room-temperature Coulomb Blockade from a Self-Assembled Molecular Nanostructure. *Phys. Rev. B: Condens. Matter Mater. Phys.* **1995,** *52*, 9071.
15. Andres, R. P.; Bein, T.; Dorogi, M.; Feng, S.; Henderson, J. I.; Kubiak, C. P.; Mahoney, W.; Osifchin, R. G.; Reifenberger, R. Coulomb Staircase" at Room Temperature in a Self-Assembled Molecular Nanostructure. *Science* **1996,** *272*, 1323–1325.
16. Reichert, J.; Ochs, R.; Beckmann, D.; Weber, H. B.; Mayor, M.; Löhneysen, H. V. Driving Current through Single Organic Molecules. *Phys. Rev. Lett.* **2002,** *88*, 176804.
17. Venkataraman, L.; Klare, J. E.; Nuckolls, C.; Hybertsen, M. S.; Steigerwald, M. L. Dependence of Single-Molecule Junction Conductance on Molecular Conformation. *Nature* **2006,** *442*, 904–907.
18. Lindsay, S. M.; Ratner, M. A. Molecular Transport Junctions: Clearing Mists. *Adv. Mater.* **2007,** *19*, 23–31.
19. Toher, C.; Sanvito, S. Efficient Atomic Self-Interaction Correction Scheme for Nonequilibrium Quantum Transport. *Phys. Rev. Lett.* **2007,** *99*, 056801.
20. Toher, C; Sanvito, S. Effects of Self-Interaction Corrections on the Transport Properties of Phenyl-Based Molecular Junctions. *Phys. Rev. B: Condens. Matter Mater. Phys.* **2008,** *77*, 155402.
21. Perdew, J. P.; Burke, K.; Ernzerhof, M. Generalized Gradient Approximation Made Simple. *Phys. Rev. Lett.* **1996,** *77*, 3865.
22. Fillippetti, A.; Spaldin, N. A. Self-Interaction Corrected Pseudopotential Scheme for Magnetic and Strongly-Correlated Systems. *Phys. Rev. B: Condens. Matter Mater. Phys.* **2003,** *67*, 125109.
23. Pemmaraju, C. D.; Archer, T.; Sanchez-Portal, D.; Sanvito, S. Atomic-Orbital Based Approximate Self-Interaction Correction Scheme for Molecules and Solids. *Phys. Rev. B: Condens. Matter Mater. Phys.* **2007,** *75*, 045101.
24. Tour, J. M.; Jones, L.; Pearson, D, L.; Lamba, J. J. S.; Burgin, T. P.; Whitesides, G. M.; Allara, D. L.; Parikh, A. N.; Atre, S. V. Self-Assembled Monolayers and Multilayers of Conjugated Thiols, .Alpha.,.Omega.-Dithiols, and Thioacetyl-Containing Adsorbates. Understanding Attachments between Potential Molecular Wires and Gold Surfaces. *J. Am. Chem. Soc.* **1995,** *117*, 9529–9534.

25. Grandbois, M.; Beyer, M.; Rief, M.; Clausen-Schaumann, H.; Gaub, H. E. How Strong Is a Covalent Bond?. *Science* **1999,** *283*, 1727–1730.
26. Kruger, D.; Fucks, H.; Rosseau, R.; Marx, D.; Parrinello, M. Pulling Monatomic Gold Wires with Single Molecules: An Ab Initio Simulation. *Phys. Rev. Lett.* **2002,** *89*, 186402.
27. Kruger, D.; Rousseau, R.; Fuchs, H.; Marx, D. Towards Mechanochemistry: Mechanically Induced Isomerizations of Thiolate-Gold Clusters. *Angew. Chem., Int. Ed.* **2003,** *42*, 2251–2253.
28. da Silva, E. Z.; Novaes, F. D.; da Silva, A. J. R.; Fazzio, A. Theoretical Study of the Formation, Evolution, and Breaking of Gold Nanowires. *Phys. Rev. B: Condens. Matter Mater. Phys.* **2004,** *69*, 115411.
29. Emberly, E. G.; Kirczenow, G. Models of Electron Transport through Organic Molecular Monolayers Self-Assembled on Nanoscale Metallic Contacts. *Phys. Rev. B: Condens. Matter Mater. Phys.* **2001,** *64*, 235412.
30. Rungger, I.; Chen, X.; Schwingenschlogl, U.; Sanvito, S. Finite-Bias Electronic Transport of Molecules in a Water Solution. *Phys. Rev. B: Condens. Matter Mater. Phys.* **2010,** *81*, 235407.
31. Hohenberg, P; Kohn, W. Inhomogeneous Electron Gas. *Phys. Rev.* **1964,** *136*, 864B.
32. Kohn, W.; Sham, L. J. Self-Consistent Equations Including Exchange and Correlation Effects. *Phys. Rev.* **1965,** *140*, 1133A.
33. Troullier, N.; Martins, J. L. Efficient Pseudopotentials for Plane-Wave Calculations. *Phys. Rev. B: Condens. Matter Mater. Phys.* **1991,** *43*, 1993.
34. Ordejón, P.; Artacho, E.; Soler, J. M. Self-Consistent Order-N Density-Functional Calculations for Very Large Systems. *Phys. Rev. B: Condens. Matter Mater. Phys.* **1996,** *53*, R10441.
35. Sánchez-Portal, D.; Ordejón, P.; Artacho, E.; Soler, J. M. Density-Functional Method for Very Large Systems with LCAO Basis Sets. *Int. J. Quantum Chem.* **1997,** *65*, 453–461.
36. Artacho, E.; Sánchez-Portal, D.; Ordejón, P.; Garcia, A.; Soler, J. M. Linear-Scaling Ab Initio Calculations for Large and Complex Systems. *Phys. Status Solidi B* **1999,** *215*, 809–817.
37. Monkhorst, H. J.; Pack, J. D. Special Points for Brillouin-Zone Integrations. *Phys. Rev. B: Solid State* **1976,** *13*, 5188.
38. Novaes, F. D.; da Silva, A. J. R.; Fazzio, A. Density Functional Theory Method for Non-Equilibrium Charge Transport Calculations: TRANSAMPA. *Braz. J. Phys.* **2001,** *36*, 799–807.
39. Rocha, A. R.; Garcia-Suarez, V.; Bailey, S. W.; Lambert, C. J.; Ferrer, J.; Sanvito, S. Spin and Molecular Electronics in Atomically Generated Orbital Landscapes. *Phys. Rev. B: Condens. Matter Mater. Phys.* **2006,** *73*, 085414.
40. M. Brandbyge, M.; Mozos, J. -L.; Ordejón, P.; Taylor, J; Stokbro, K. Density-Functional Method for Nonequilibrium Electron Transport. *Phys. Rev. B: Condens. Matter Mater. Phys.* **2002,** *65*, 165401.
41. Taylor, J.; Guo, H.; Wang, J. Ab Initio Modeling of Quantum Transport Properties of Molecular Electronic Devices. *Phys. Rev. B: Condens. Matter Mater. Phys.* **2001,** *63*, 245407.
42. Xue, Y.; Datta, S.; Ratner, M. A. First-Principles Based Matrix Green's Function Approach to Molecular Electronic Devices: General Formalism. *Chem. Phys.* **2002,** *281*, 151–170.
43. Perdew, J. P.; Zunger, A. Self-Interaction Correction to Density-Functional Approximations for Many-Electron Systems. *Phys. Rev. B: Condens. Matter Mater. Phys.* **1981,** *23*, 5048.